

Supramolecular Architectures of Four New Transition Metal Complexes with 3-[4-(Carboxymethoxy)phenyl]propanoic Acid and N-[4-(Carboxymethoxy)phenyl]iminodiacetic Acid

Chong-Bo Liu,*^[a] Hui-Liang Wen,^[b] Yun-Nan Gong,^[a] Xiao-Ming Liu,^[a] and Sheng-Shui Tan^[b]

Keywords: 3-[4-(carboxymethoxy)phenyl]propanoic acid; N-[4-(carboxymethoxy)phenyl]iminodiacetic acid; Supramolecular chemistry; Copper; Cobalt; Nickel

Abstract. Four new transition metal complexes: $[\text{Cu}(\text{Hcппa})_2(\text{H}_2\text{O})_2]$ (**1**), $[\text{Co}_2(\text{cppa})_2(\text{H}_2\text{O})_{10}]$ (**2**), $[\text{Co}_3(\text{cpia})_2(\text{H}_2\text{O})_8] \cdot 2\text{H}_2\text{O}$ (**3**) and $[\text{Ni}_3(\text{cpia})_2(\text{H}_2\text{O})_{12}] \cdot 6\text{H}_2\text{O}$ (**4**) { $\text{H}_2\text{cppa} = 3\text{-}(4\text{-}(\text{carboxymethoxy)phenyl)propanoic acid}$; $\text{H}_3\text{cpia} = N\text{-}[4\text{-}(\text{carboxymethoxy)phenyl)iminodiacetic acid}$ } were synthesized and characterized. Complexes **1** and **2** show mononuclear structures, complexes **3** and **4** exhibit dinuclear

structures. All complexes extend to 3D supramolecular networks through hydrogen bonds, of which complexes **3** and **4** display microporous structures. In complexes **2–4** the water clusters are trapped by the cooperative association of coordinate interactions as well as hydrogen bonds, forming different 1D metal–water chain structures. Thermal stabilities of complexes **1–4** were discussed.

Introduction

Recently, much attention has been paid to the design and synthesis of high-dimensional supramolecular complexes because of their ability to form frameworks with various structures, as well as their interesting magnetic, optical, and porosity properties [1–11]. Hydrogen bonding, as major intermolecular force, is usually applied to increase the structural dimensionality of supramolecular systems. Water molecules and carboxylic acids as good hydrogen-bond donors and acceptors have been widely used to construct supramolecular complexes. Up to now, much work has been done about the research of hydrogen bonding in discrete water clusters (H_2O_n , ($n = 2\text{--}18$), as well as polymeric water clusters [12–14]. Unfortunately, only very limited information has been obtained about metal–water clusters not only including hydrogen bonding interactions between water molecules, but also coordination interaction between metal atoms and water clusters [15], although the structural study of them could provide valuable information for unraveling the mechanism in energy-transduction or proton conduction.

On the other hand, exploiting flexible carboxylate ligands with suitable spacers to construct supramolecular complexes with porous structures also has been widely investigated [16–20]. H_2cppa and H_3cpia ligands exhibit several interesting

characteristics: (1) Both contain one phenyl ring and one oxoacetate group, in addition, the H_2cppa ligand has one propionate function and the H_3cpia ligand has one $-\text{N}(\text{CH}_2\text{COOH})_2$ group, so they not only display the characteristics of flexibility and rigidity, but also have long spacers in comparison with the corresponding ring-shaped multidentate carboxylates [21–24], such as 1,4-benzenedicarboxylate, which will help to form porous structures. (2) The two ligands have multiple coordination sites and can provide various bridging and chelating coordination modes displayed by the $-\text{OCH}_2\text{COOH}$, $-\text{CH}_2\text{CH}_2\text{COOH}$ and $-\text{N}(\text{CH}_2\text{COOH})_2$ groups to construct different structures. (3) The coordination sites of the two ligands can be used as hydrogen-bond acceptors as well as hydrogen-bond donors, which assist in the generation of high-dimensional supramolecular networks.

In view of these factors, we were working on the synthesis of supramolecular complexes with H_2cppa and H_3cpia ligands, and reported the structures of three complexes containing the H_2cppa compound, $[\text{M}(\text{H}_2\text{O})_4(4,4'\text{-bpy})][\text{cppa}]$ ($\text{M} = \text{Co, Ni, Zn}$; $4,4'\text{-bpy} = 4,4'\text{-bipyridine}$), in which the H_2cppa compounds are completely deprotonated but remain uncoordinated to metal ions [25–27]. Except the above three complexes, no other structural characterization of H_2cppa complexes were reported. To the best of our knowledge, up to now there are also no reports of H_3cpia ligand. Accordingly, in the present work, we report the syntheses and characterizations of four new transition metal complexes with two kinds of multicarboxylate ligands: $[\text{Cu}(\text{Hcппa})_2(\text{H}_2\text{O})_2]$ (**1**), $[\text{Co}_2(\text{cppa})_2(\text{H}_2\text{O})_{10}]$ (**2**), $[\text{Co}_3(\text{cpia})_2(\text{H}_2\text{O})_8] \cdot 2\text{H}_2\text{O}$ (**3**), and $[\text{Ni}_3(\text{cpia})_2(\text{H}_2\text{O})_{12}] \cdot 6\text{H}_2\text{O}$ (**4**).

* Prof. Dr. C.-B. Liu
E-Mail: cbliu2002@163.com

[a] School of Environment and Chemical Engineering
Nanchang Hangkong University
Nanchang 330063, P. R. China

[b] State Key Laboratory of Food Science and Technology
Nanchang University
Nanchang 330047, P. R. China

Results and Discussion

Structural Descriptions

[Cu(H₂cппa)₂(H₂O)₂] (1)

Single crystal X-ray diffraction analysis reveals that complex **1** has a mononuclear structure, as shown in Figure 1. The Cu^{II} ion is hexacoordinated by two carboxylate oxygen atoms and two ether oxygen atoms from two H₂cппa⁻ anions, and two water oxygen atoms. It lies on an inversion center and has a slightly distorted octahedral arrangement. Every H₂cппa ligand loses one proton and coordinates to one Cu^{II} ion in a bidentate mode (Scheme 1a). Through dual O₃–H₃···O₂ hydrogen bonds between unprotonated carboxyl groups adjacent [Cu(H₂cппa)₂] units are linked to a 1D chain structure, which is further joined

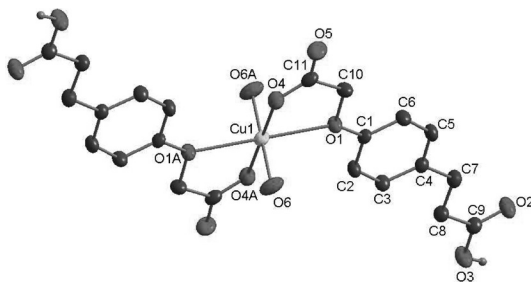
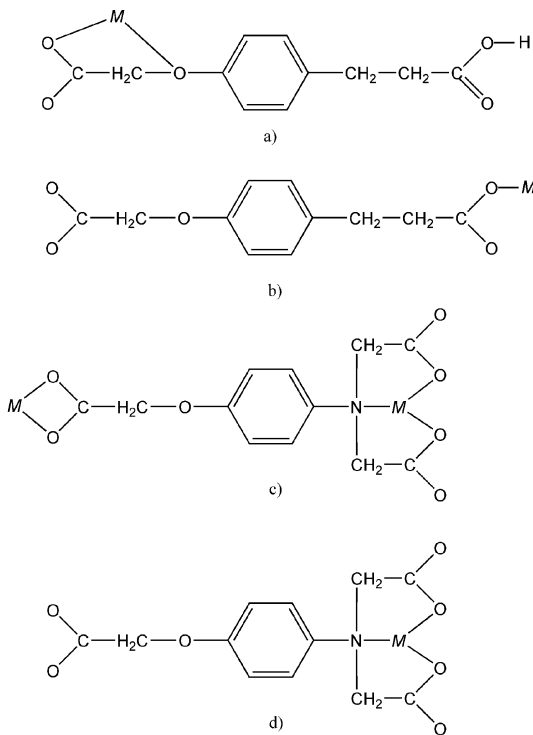


Figure 1. Coordination environment of the Cu^{II} ion in complex **1** with 50 % thermal ellipsoids. All hydrogen atoms except the one of the carboxyl group are omitted for clarity. Symmetry operation: A = $-x+1, -y+2, -z+1$.



Scheme 1. Coordination modes of H₂cппa and H₃cpia ligands in complexes **1–4**.

to a 2D layer containing regular parallelogram grids with dimensions of $6.7 \times 23.0 \text{ \AA}^2$ based on the Cu···Cu distance by O₆–H_{1W}···O₅ hydrogen bonds between uncoordinated carboxylate oxygen atoms and coordinated water molecules along the *a* axis. Finally, O₆–H_{2W}···O₅ and C₆–H_{6A}···O₃ hydrogen bonds among adjacent layers link complex **1** to a 3D supramolecular structure, as shown in Figure 2.

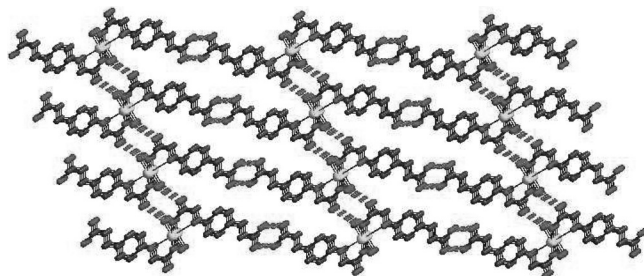


Figure 2. 3D Supramolecular structure of complex **1** viewed along the *a* axis, the hydrogen bonding interactions are represented by dashed lines.

[Co₂(cппa)₂(H₂O)₁₀] (2)

As shown in Figure 3, each Co^{II} ion in complex **2** is hexacoordinated by one carboxylate oxygen atom from one cппa²⁻ anion and five water oxygen atoms, the coordination environments of Co(1) and Co(2) are similar, but the bond lengths of Co(1)–O and Co(2)–O are different, the Co(1)–O distances are in the range of 2.051–2.134 Å, and Co(2)–O distances are in the range of 2.044–2.170 Å. Differing from **1**, the carboxyl groups of H₂cппa ligand are completely deprotonated in **2**, and the cппa²⁻ anions display a monodentate mode (see Scheme 1b). The O–H···O hydrogen bonds between carboxylate oxygen atoms and coordinated water molecules link [Co₁(cппa)(H₂O)₅]²⁺ and [Co₂(cппa)(H₂O)₅]²⁺ units to form the 2D layer structures, which contain numerous parallelograms with dimensions of ca. $5.1 \times 18.2 \text{ \AA}^2$ and $5.1 \times 17.3 \text{ \AA}^2$ based on the nearest distance of the Co^{II} ions, respectively, as shown in Figure 4a and Figure 4c. In [Co₁(cппa)(H₂O)₅]²⁺ layers, O₁, O₂, O₃, and Co₁²⁺ ions form a metal–water chain by coordination interactions and hydrogen bonds; similarly in [Co₂(cппa)(H₂O)₅]²⁺ layers, O₆, O₇, O₈, O₉, and Co₂²⁺ ions form a metal–water chain, too; these two metal–water chains are linked through O₃–H₆···O₇ hydrogen bonds, resulting in an infinite ladder-like metal–water chain (Figure 5a), which join the [M(cппa)(H₂O)₅] (*M* = Co₁, Co₂) layers to a 3D supramolecular structure, as shown in Figure 4b.

[Co₃(cpia)₂(H₂O)₈]·2H₂O (3)

There are two crystallographically independent Co^{II} ions in the asymmetric unit of **3** (see Figure 6a). Each Co₁ ion has a center of symmetry and is coordinated by six water molecules, Co₂ is hexacoordinated by one nitrogen atom and four carboxylate oxygen atoms of two cpia³⁻ anions and one water oxygen atom, the ratio of Co₁:Co₂ is 1:2. H₃cpia ligands are com-

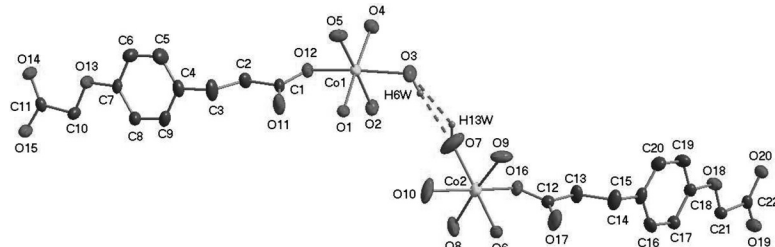


Figure 3. Coordination environment of Co^{II} ions in complex **2** with 50 % thermal ellipsoids. All hydrogen atoms except those of the $\text{O}-\text{H}\cdots\text{O}$ groups are omitted for clarity.

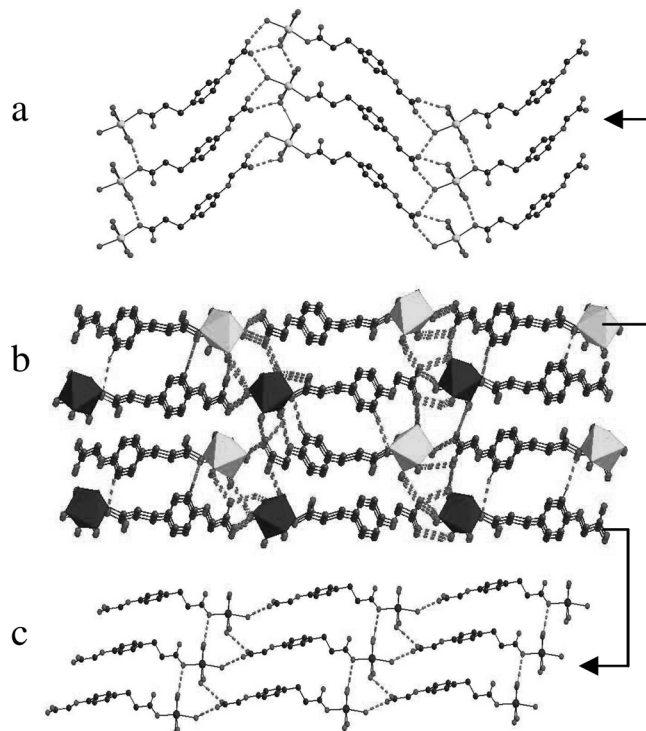


Figure 4. (a) Views of the 2D network constructed by Co_2 ions along the a axis; (b) The 3D supramolecular structure of complex **2** along the b axis; (c) Views of the 2D network constructed by Co_1 ions along the a axis; the hydrogen bonding interactions are represented by dashed lines.

pletely deprotonated and show bis-N,O-chelating and O,O-chelating coordination modes (as shown in Scheme 1c). Intramolecular $\text{O}-\text{H}\cdots\text{O}$ hydrogen bonds between carboxylate oxygen atoms and coordinated water molecules link Co_1 and Co_2 ions of an asymmetric unit, as shown in Figure 6a. Two H_3cpia ligands join two Co_2^{2+} ions to form a $[\text{Co}_2(\text{cpia})_2]^{2-}$ building block with $\text{Co}_2\cdots\text{Co}_2$ distance of 10.31 Å. Every $[\text{Co}_2(\text{cpia})_2]^{2-}$ unit is bridged by six adjacent $[\text{Co}_2(\text{cpia})_2]^{2-}$ units through $\text{O}_4-\text{H}7\text{W}\cdots\text{O}_{10}$, $\text{O}_4-\text{H}8\text{W}\cdots\text{O}_{10}$, $\text{C}_5-\text{H}5\cdots\text{O}_6$, and $\text{C}_8-\text{H}8\cdots\text{O}_8$ hydrogen bonds (see Table 3) to form a 3D supramolecular network. The 3D supramolecular network shows microporous structure with infinite cavities of ca. $5.7 \times 9.7 \text{ \AA}^2$ defined by the nearest distance of the $\text{Co}_2(\text{II})$ ions along the a axis, and another building blocks

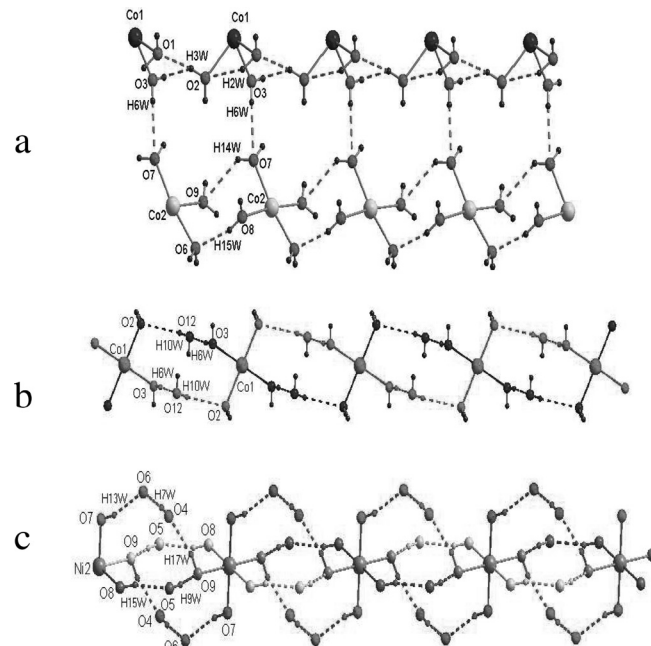


Figure 5. (a) View of a 1D metal–water chain of complex **2**; (b) View of a 1D metal–water chain containing two single stranded helices in complex **3**. (c) View of a 1D metal–water chain containing four single stranded helices in complex **4**.

$[\text{Co}_1(\text{H}_2\text{O})_6]^{2+}$ are enclathrated in the cavities through $\text{O}_{\text{water}}-\text{H}\cdots\text{O}_{\text{water}}$ hydrogen bonds, as shown in Figure 6b. Co_1-O_3 and Co_1-O_2 coordination interactions combine with $\text{O}_3-\text{H}6\text{W}\cdots\text{O}_{12}$ and $\text{O}_1-\text{H}10\text{W}\cdots\text{O}_2$ hydrogen bonds between uncoordinated and coordinated water molecules, resulting in a metal–water chain with two single stranded helices, as shown in Figure 5b.

$[\text{Ni}_3(\text{cpia})_2(\text{H}_2\text{O})_{12}] \cdot 6\text{H}_2\text{O}$ (**4**)

As shown in Figure 7a, complex **4** has a dinuclear structure with two crystallographically independent Ni^{II} ions. Ni_1 is hexacoordinated by one nitrogen atom and two carboxylate oxygen atoms of one cpia³⁻ anion and three water oxygen atoms, whereas Ni_2 is hexacoordinated to six water molecules, the ratio of $\text{Ni}_1:\text{Ni}_2$ is 2:1. H_3cpia ligands are completely deprotonated and adopt a bis-N,O-chelating coordination mode, as

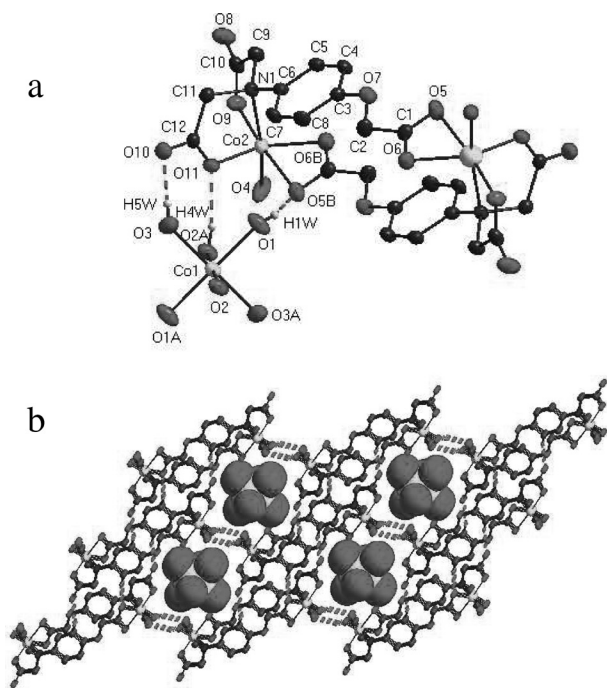


Figure 6. (a) Coordination environments of the Co^{II} ions in complex 3 with 50 % thermal ellipsoids, all hydrogen atoms except those of the $\text{O}-\text{H}\cdots\text{O}$ groups are omitted for clarity. Symmetry operations: A = $-x+1, -y+1, -z+1$; B = $-x+1, -y+1, -z+2$. (b) The 3D supramolecular structure of 3 along the a axis, indicating the cavities occupied by the building blocks $[\text{Co}(\text{H}_2\text{O})_6]^{2+}$, which are displayed in space-filling model. The hydrogen bonding interactions are represented by dashed lines.

shown in Scheme 1d, one H_3cpia ligand only links one Ni^{II} ion. Through $\text{O}-\text{H}\cdots\text{O}$ hydrogen bonds between the carboxylate oxygen atoms and coordinated water molecules two H_3cpia ligands link two Ni^{II} ions to form a $[\text{Ni}_2(\text{cpia})_2]^{2-}$ building block (see Figure 7a) with a $\text{Ni}^{II}\cdots\text{Ni}^{II}$ distance of 13.0 Å, which is slightly longer than the $\text{Co}^{II}\cdots\text{Co}^{II}$ distance (10.31 Å) of $[\text{Co}_2(\text{cpia})_2]^{2-}$ building block in complex 3. Similar to 3, each $[\text{Ni}_2(\text{cpia})_2]^{2-}$ unit is bridged by six adjacent $[\text{Ni}_2(\text{cpia})_2]^{2-}$ units through $\text{O}_2-\text{H}3\text{W}\cdots\text{O}_{13}$, $\text{O}_2-\text{H}4\text{W}\cdots\text{O}_{11}$, and $\text{O}_3-\text{H}5\text{W}\cdots\text{O}_{16}$ hydrogen bonds (see Table 3) to form a 3D supramolecular network, which has infinite cavities of ca. $8.3 \times 10.2 \text{ \AA}^2$ along the a axis, and another kind of building blocks $[\text{Ni}_2(\text{H}_2\text{O})_6]^{2+}$ are enclathrated in the cavities through hydrogen bonds, as shown in Figure 7b. Three uncoordinated water molecules (O_4 , O_5 , and O_6) and three coordinated water molecules (O_7 , O_8 , and O_9) are associated to discrete hexamer clusters by $\text{O}_7-\text{H}13\text{W}\cdots\text{O}_6$, $\text{O}_6\cdots\text{H}7\text{W}-\text{O}_4$, $\text{O}_4-\text{H}7\text{W}\cdots\text{O}_9$, $\text{O}_9\cdots\text{H}9\text{W}-\text{O}_5$, and $\text{O}_5\cdots\text{H}15\text{W}-\text{O}_8$ hydrogen bonds with an average $\text{O}\cdots\text{O}$ distance of 2.788 Å, which is close to corresponding value of 2.759 Å in ice I_h [28]. Adjacent hexamers are further linked to form a metal–water chain by Ni_2-O_7 , Ni_2-O_8 , and Ni_2-O_9 coordination, where four single-stranded helices can be observed, as shown in Figure 5c.

Syntheses of the Complexes

The reaction conditions for the synthesis of complex 2 are similar to those of the synthesis of $[\text{Co}(\text{H}_2\text{O})_4(4,4'\text{-bpy})][\text{cpfa}]$ (5), which was reported previously to some extends [27]. The difference is that 4,4'-bipyridine (0.1 mmol) in complex 5 was

Table 1. Crystal data for complexes 1–4.

	1	2	3	4
Empirical formula	$\text{C}_{22}\text{H}_{26}\text{CuO}_{12}$	$\text{C}_{22}\text{H}_{40}\text{Co}_2\text{O}_{20}$	$\text{C}_{24}\text{H}_{40}\text{Co}_3\text{N}_2\text{O}_{24}$	$\text{C}_{24}\text{H}_{56}\text{N}_2\text{Ni}_3\text{O}_{32}$
Formula weight / g·mol ⁻¹	545.97	742.40	917.36	1060.84
T / K	291(2)	291(2)	291(2)	291(2)
Crystal system	Triclinic	Orthorhombic	Triclinic	Triclinic
Space group	$P\bar{1}$	Pca_2_1	$P\bar{1}$	$P\bar{1}$
<i>a</i> / Å	5.337(11)	19.489(18)	7.626(12)	7.218(13)
<i>b</i> / Å	6.710(14)	5.115(5)	9.670(15)	10.478(18)
<i>c</i> / Å	16.386(3)	29.999(3)	12.494(19)	13.498(2)
α / °	87.147(2)	90	85.165(2)	96.500(2)
β / °	82.173(2)	90	76.429(2)	90.896(2)
γ / °	73.132(2)	90	77.987(2)	96.512(2)
<i>V</i> / Å ³	556.3(2)	2990.6(5)	875.4(2)	1007.2(3)
<i>Z</i>	1	4	1	1
θ range / °	2.51–25.49	2.49–25.50	2.68–27.50	2.84–22.18
μ / mm ⁻¹	1.050	1.197	1.502	1.499
<i>F</i> (000)	283	1544	471	554
<i>D</i> _c / mg·m ⁻³	1.630	1.649	1.740	1.749
Goodness-of-fit on <i>F</i> ²	1.090	0.990	1.000	1.021
No. data collected	4238	21098	7833	7597
No. unique data	2057	5543	3949	3730
<i>R</i> _{int}	0.0138	0.0422	0.0342	0.0448
<i>R</i> ₁ , <i>wR</i> ₂ [<i>I</i> > 2σ(<i>I</i>)]	0.0253, 0.0668	0.0516, 0.1213	0.0400, 0.0798	0.0449, 0.0873
<i>R</i> ₁ , <i>wR</i> ₂ (all data)	0.0268, 0.0679	0.0565, 0.1246	0.0694, 0.0946	0.0780, 0.1030
Largest diff. peak and hole / e·Å ⁻³	0.248, -0.327	1.729, -0.393	0.434, -0.348	0.453, -0.600

Table 2. Selected bond lengths /Å for complexes **1–4**.

1		Cu(1)–O(4)	
Cu(1)–O(1)	2.420(13)		1.963(13)
Cu(1)–O(6)	1.948(14)		
2			
Co(1)–O(1)	2.103(3)	Co(2)–O(6)	2.134(3)
Co(1)–O(2)	2.124(4)	Co(2)–O(7)	2.171(4)
Co(1)–O(3)	2.132(4)	Co(2)–O(8)	2.097(4)
Co(1)–O(4)	2.109(4)	Co(1)–O(9)	2.083(4)
Co(1)–O(5)	2.087(4)	Co(2)–O(10)	2.066(4)
Co(1)–O(12)	2.051(3)	Co(2)–O(16)	2.045(4)
3^{a)}			
Co(1)–O(1)	2.078(2)	Co(2)–O(6) ^{#1}	2.081(2)
Co(1)–O(2)	2.102(2)	Co(2)–O(9)	2.011(2)
Co(1)–O(3)	2.093(2)	Co(2)–O(11)	1.997(2)
Co(2)–O(4)	2.030(2)	Co(2)–N(1)	2.306(3)
Co(2)–O(5) ^{#1}	2.304(2)		
4			
Ni(1)–O(1)	2.028(3)	Ni(1)–N(1)	2.181(3)
Ni(1)–O(2)	2.072(3)	Ni(2)–O(7)	2.022(3)
Ni(1)–O(3)	2.047(3)	Ni(2)–O(8)	2.035(3)
Ni(1)–O(10)	2.047(3)	Ni(2)–O(9)	2.085(3)
Ni(1)–O(12)	2.023(3)		

a) For **3**: Symmetry operation: #1 $-x+1, -y+1, -z+2$.

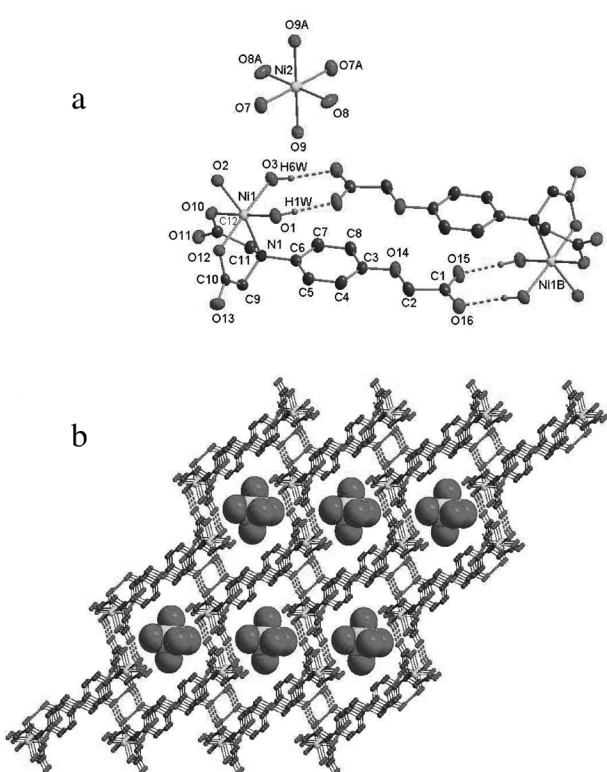


Figure 7. (a) Coordination environments of Ni^{II} ions in complex **4** with 50 % thermal ellipsoids, all hydrogen atoms except that of the O–H···O groups are omitted for clarity. Symmetry operations: A = $-x+1, -y+2, -z$; B = $-x+2, -y, -z+1$. (b) The 3D supramolecular structure of complex **4** along the *a* axis, indicating the cavities occupied by the building blocks [Ni(H₂O)₆]²⁺, which are displayed in space-filling model. The hydrogen bonding interactions are represented by dashed lines.

replaced by NaOH (0.3 mL, 0.65 M) in complex **2**, which led to quite different structures. Although the carboxyl groups of H₂cppa ligands are completely deprotonated in complexes **2** and **5**, in complex **2** one cppa²⁻ ligand is coordinated to one Co²⁺ ion, whereas in complex **5** the cppa²⁻ ions only act as a charge balance and hydrogen bonds acceptors to form O–H···O hydrogen bonds with water molecules, which join the chain structure of [Co(4,4'-bpy)·4H₂O] blocks into a 3D supramolecular structure.

Complex **1** was synthesized by a hydrothermal reaction under high pressure, whereas complexes **2–4** were obtained under autogenous pressure. Low pressure may be available for the coordination of water molecules to metal ions in the reaction systems: in complex **1** only two water molecules are involved in coordination; whereas in complexes **2–4** ca. 8–12 water molecules take part in coordination, different water clusters are trapped by the cooperative association of coordinate interactions as well as hydrogen bonds, which result in different 1D metal–water chain structures in complexes **2–4**.

From the structural descriptions of complexes **1–4**, it can be seen that although H₂cppa and H₃cpia ligands have similar characteristics, and all metal ions in complexes **1–4** are hexacoordinate, complexes **1–4** display different supramolecular networks, and only complexes **3** and **4** show microporous structures. In complexes **1** and **2**, the H₂cppa ligands show monodentate and bidentate coordination modes (as shown in Scheme 1a and Scheme 1b), one H₂cppa ligand only links one metal ion. In complexes **3** and **4**, the H₃cpia ligands adopt tridentate and pentadentate coordination modes (as shown in Scheme 1c, Scheme 1d), one H₃cpia ligand links one or two metal ions, but two H₃cpia ligands join two metal ions to form a dimeric unit by coordination bonds and/or hydrogen bonds;

with the help of hydrogen bonds with suitable direction. Each dimeric unit is bridged with six adjacent units to form 3D supramolecular networks with microporous structure. So it can be concluded that coordination modes of ligands and hydrogen bonds have profound influences on the supramolecular architecture of the title complexes, and hydrogen bonds, especially its direction is crucial to the microporous supramolecular construction of complexes **3** and **4**.

Thermogravimetric Analyses

Thermogravimetric analyses of the four complexes were carried out to examine their thermal stabilities. For complex **1**, the first weight loss of 6.4 % from 60 °C to 195 °C corresponds to the loss of two coordinated water molecules per mononuclear unit (calcd. 6.6 %). Increasing temperature led to further decomposition and the final pyrolysis was completed at 758 °C, to yield a powder of CuO (found 14.2 %, calcd. 14.6 %). For complex **2**, the first weight loss (ten coordinated water molecules) of 23.8 % (calcd. 24.3 %) was observed from 50 °C to 121 °C, leaving a framework of $[Co_2(cpppa)_2]$. The dehydrated compound is stable up to 288 °C, the second weight loss of 54.9 % (calcd. 55.5 %) from 288 °C to 850 °C corresponds to the burning of the organic groups, the final residual is CoO.

Complex **3** underwent the first weight loss of 19.1 % from 50 °C to 155 °C, corresponding to the loss of two lattice water molecules and eight coordinated water molecules per formula unit (calcd. 19.6 %), leaving a framework of $[Co_3(copia)_2]$. Further decomposition of **3** occurred above 370 °C, and was completed at 865 °C, to yield a powder of CoO (found 25.1 %, calcd. 24.5 %). The TGA curve of complex **4** shows that the first weight loss of 30.1 %, which occurred at 58 °C and ended at 133 °C, corresponds to the loss of six lattice water molecules and twelve coordinated water molecules (calcd. 30.5 %). Afterwards, increasing temperature led to further decomposition, which began at 320 °C and the final pyrolysis was completed at 775 °C with the residual NiO in 20.9 % yield (calcd. 21.2 %).

Conclusions

Four new transition metal complexes with different supramolecular networks were obtained by using the multicarboxylate ligands with suitable spacers and characteristics of both flexibility and rigidity. Water, H₂cpppa, and H₃copia ligands are excellent hydrogen bonding donors and acceptors, which help to extend the 0D structures of complexes **1–4** to 3D supramolecular structures. The results of single-crystal X-ray diffraction demonstrate that metal ions, coordination modes of ligands, and hydrogen bonds have important effect on the supramolecular architectures of the title complexes. Thermogravimetric analyses show that the thermal stabilities of complexes **1–4** are relatively low.

Experimental Section

Materials and Methods: The ligands H₂cpppa and H₃copia were synthesized using an improved method described elsewhere [29]. All the

other chemical reagents were obtained commercially and were used without further purification. The elemental analysis of C, H, and N were carried out with an Elementar Vario EL analyzer. The IR spectra were recorded with a Nicolet Avatar 360 FT-IR spectrometer using the KBr pellet technique. Thermogravimetric curves were recorded with a ZRY-2P Thermal Analyzer.

Synthesis of Complexes **1–4**

[Cu(Hcppa)₂(H₂O)₂] (1): A mixture of CuSO₄·5H₂O (0.025 g, 0.1 mmol), H₂cpppa (0.022 g, 0.1 mmol), NaOH (0.2 mL, 0.65 M), and distilled water (10 mL) was sealed in a Teflon-lined stainless reactor (23 mL) and heated 90 °C for 72 h under autogenous pressure. Blue block crystals were obtained. Yield 32.5 %. C₂₂H₂₆CuO₁₂: calcd. C 48.40; H 4.80 %; found: C 48.71; H 4.95 %. IR (KBr): $\tilde{\nu}$ = 3032 w, 1717 s, 1637 s, 1519 s, 1437 w, 1346 m, 1279 m, 1216 m, 1061 s, 949 s, 832 s, 793 w, 675 m cm⁻¹.

[Co₂(cpppa)₂(H₂O)₁₀] (2): A mixture of CoCl₂·6H₂O (0.024 g, 0.1 mmol), H₂cpppa (0.022 g, 0.1 mmol), NaOH (0.2 mL, 0.65 M), and distilled water was sealed in an unfiled test-tube (15 mL) and heated at 90 °C for 5 h under autogenous pressure. Red tetragonal block crystals were obtained. Yield 27.5 %. C₂₂H₄₀Co₂O₂₀: calcd. C 35.59; H 5.43 %; found: C 35.84; H 5.66 %. IR (KBr): $\tilde{\nu}$ = 3605 w, 1780 m, 1650 m, 1580 w, 1466 vs, 1375 s, 1272 w, 1156 m, 1057 m, 950 w, 840 w, 722 vs, 630 w cm⁻¹.

[Co₃(copia)₂(H₂O)₈]·2H₂O (3): The synthesis of **3** was similar to that of **2**, except that H₃copia (0.028 g, 0.1 mmol) was used instead of H₂cpppa. Red block crystals were obtained. Yield 23.5 %. C₂₄H₄₀N₂Co₃O₂₄: calcd. C 31.42; H 4.40; N 3.05 %; found: C 31.72; H 4.64; N 3.26 %. IR (KBr): $\tilde{\nu}$ = 3487 w, 1615 s, 1560 m, 1514 m, 1420 s, 1334 m, 1234 s, 1186 w, 1118 w, 1074 m, 977 m, 912 m, 801 w, 685 m cm⁻¹.

[Ni₃(copia)₂(H₂O)₁₂]·6H₂O (4): The synthesis of **4** was the same as that of **3**, except that Ni(NO₃)₂·6H₂O was used instead of CoCl₂·6H₂O. Green stick crystals were obtained. Yield 25.5 %. C₂₄H₅₆N₂Ni₃O₃₂: calcd. C 27.33; H 5.32; N 2.64 %; found: C 27.35; H 5.59; N 2.95 %. IR (KBr): $\tilde{\nu}$ = 3415 s, 1618 s, 1562 m, 1513 w, 1419 m, 1331 w, 1242 m, 1188 w, 1142 w, 1061 w, 917 w, 807 m, 701 w, 667 w cm⁻¹.

X-ray Diffraction Analyses

The X-ray single-crystal data of **1–4** were collected with a Bruker SMART 1000 CCD area detector diffractometer with graphite-monochromated Mo-K_α radiation (λ = 0.71073 Å). Semi-empirical absorption corrections were applied to all four complexes using the SADABS program. The structures were solved by direct methods using the program SHELXS 97 [30] and refined by full-matrix least-squares on F^2 using SHELXL 97 [31]. All non-hydrogen atoms were refined anisotropically. Hydrogen atoms were placed in geometrically calculated positions. Experimental details for X-ray data collection of **1–4** are presented in Table 1, selected bond lengths are listed in Table 2, and the types of hydrogen bonds are listed in Table 3.

The crystallographic data for the structures in this paper have been deposited with the Cambridge Crystallographic Data Centre, CCDC, 12 Union Road, Cambridge CB2 1EZ, UK. Copies of the data can be obtained free of charge on quoting the depositary numbers CCDC-752379, -752380, -752381, and -752382 for **1–4** (Fax: +44-1223-336-033; E-Mail: deposit@ccdc.cam.ac.uk or www: http://www.ccdc.cam.ac.uk).

Table 3. Types of hydrogen bonds in complexes **1–4**.

D–H	<i>d</i> (D–H)	<i>d</i> (H···A)	\angle (DHA)	<i>d</i> (D···A)	A
1					
O(3)–H(3)	0.82	1.83	173.7	2.651(2)	O(2)[− <i>x</i> −1, − <i>y</i> +1, − <i>z</i>]
O(6)–H(1W)	0.81	1.85	173.3	2.658(2)	O(5) [<i>x</i> , <i>y</i> −1, <i>z</i>]
O(6)–H(2W)	0.81	2.06	170.2	2.857(2)	O(4) [− <i>x</i> +2, − <i>y</i> +2, − <i>z</i> +1]
C(6)–H(6A)	0.93	2.45	149.0	3.285(3)	O(3) [<i>x</i> +1, <i>y</i> +1, <i>z</i>]
2					
O(1)–H(1W)	0.83	1.83	145.8	2.567(5)	O(11)
O(1)–H(2W)	0.90	2.17	116.7	2.698(5)	O(19) [− <i>x</i> , − <i>y</i> +2, <i>z</i> +1/2]
O(1)–H(2W)	0.90	2.36	131.1	3.028(5)	O(2)
O(2)–H(3W)	0.83	2.18	137.0	2.841(5)	O(1) [<i>x</i> , <i>y</i> +1, <i>z</i>]
O(2)–H(4W)	0.88	2.06	143.9	2.819(5)	O(14) [− <i>x</i> +1/2, <i>y</i> −1, <i>z</i> −1/2]
O(3)–H(5W)	0.83	1.93	161.6	2.727(5)	O(15) [− <i>x</i> +1/2, <i>y</i> −2, <i>z</i> −1/2]
O(3)–H(6W)	0.83	2.25	174.9	3.078(6)	O(7)
O(4)–H(7W)	0.83	1.96	163.4	2.768(5)	O(20) [− <i>x</i> +1/2, <i>y</i> −1, <i>z</i> +1/2]
O(5)–H(9W)	0.83	2.38	129.3	2.975(5)	O(20) [− <i>x</i> +1/2, <i>y</i> −1, <i>z</i> +1/2]
O(5)–H(10W)	0.83	2.02	174.4	2.847(5)	O(12) [<i>x</i> , <i>y</i> −1, <i>z</i>]
O(6)–H(11W)	0.83	1.88	143.7	2.597(5)	O(17)
O(6)–H(12W)	0.84	1.94	156.3	2.723(5)	O(15) [− <i>x</i> , − <i>y</i> +2, <i>z</i> −1/2]
O(7)–H(13W)	0.83	2.27	148.0	3.005(7)	O(14) [− <i>x</i> +1/2, <i>y</i> −2, <i>z</i> −1/2]
O(7)–H(14W)	0.83	2.44	149.4	3.176(6)	O(14) [− <i>x</i> +1/2, <i>y</i> −1, <i>z</i> −1/2]
O(7)–H(14W)	0.83	2.44	137.2	3.097(7)	O(9) [<i>x</i> , <i>y</i> +1, <i>z</i>]
O(8)–H(15W)	0.83	1.97	159.6	2.763(5)	O(6) [<i>x</i> , <i>y</i> +1, <i>z</i>]
O(8)–H(16W)	0.83	1.94	166.6	2.755(5)	O(20) [− <i>x</i> , − <i>y</i> +2, <i>z</i> +1/2]
O(9)–H(17W)	0.83	1.98	175.6	2.808(6)	O(16) [<i>x</i> , <i>y</i> −1, <i>z</i>]
O(9)–H(18W)	0.82	2.00	156.4	2.775(6)	O(14) [− <i>x</i> +1/2, <i>y</i> −2, <i>z</i> −1/2]
O(10)–H(19W)	0.83	1.84	176.5	2.666(6)	O(19) [− <i>x</i> , − <i>y</i> +2, <i>z</i> +1/2]
O(10)–H(20W)	0.83	2.12	156.4	2.900(6)	O(20) [− <i>x</i> , − <i>y</i> +1, <i>z</i> +1/2]
C(6)–H(6A)	0.93	2.54	172.0	3.466(7)	O(16)[1/2− <i>x</i> , 1+ <i>y</i> , 1/2+ <i>z</i>]
C(19)–H(19)	0.93	2.53	162.0	3.424(7)	O(12) [1/2− <i>x</i> , <i>y</i> , −1/2+ <i>z</i>]
3					
O(1)–H(1W)	0.83	1.98	163.6	2.782(3)	O(5) [− <i>x</i> +1, − <i>y</i> +1, − <i>z</i> +2]
O(1)–H(2W)	0.83	1.95	165.2	2.752(3)	O(8) [<i>x</i> , <i>y</i> −1, <i>z</i>]
O(2)–H(3W)	0.83	1.92	164.7	2.730(3)	O(9) [<i>x</i> , <i>y</i> −1, <i>z</i>]
O(2)–H(4W)	0.83	1.99	169.9	2.813(3)	O(11) [− <i>x</i> +1, − <i>y</i> +1, − <i>z</i> +1]
O(3)–H(5W)	0.87	1.97	172.6	2.835(3)	O(10)
O(3)–H(6W)	0.83	1.92	174.6	2.754(4)	O(12) [<i>x</i> −1, <i>y</i> , <i>z</i>]
O(4)–H(7W)	0.83	2.14	154.3	2.904(3)	O(10) [− <i>x</i> +1, − <i>y</i> +2, − <i>z</i> +1]
O(4)–H(8W)	0.83	1.82	169.6	2.639(3)	O(10) [<i>x</i> +1, <i>y</i> , <i>z</i>]
O(12)–H(9W)	0.83	2.64	112.2	3.055(4)	O(7) [<i>x</i> +1, <i>y</i> , <i>z</i> −1]
O(12)–H(10W)	0.83	2.47	147.2	3.204(4)	O(2) [− <i>x</i> +1, − <i>y</i> +1, − <i>z</i> +1]
C(5)–H(5)	0.93	2.39	166.0	3.301(4)	O(6) [<i>x</i> , <i>y</i> +1, <i>z</i>]
C(8)–H(8)	0.93	2.35	152.0	3.209(4)	O(8) [<i>x</i> , <i>y</i> −1, <i>z</i>]
4					
O(1)–H(1W)	0.83	1.81	163.9	2.612(4)	O(15) [− <i>x</i> +2, − <i>y</i> , − <i>z</i> +1]
O(1)–H(2W)	0.83	1.95	170.7	2.768(4)	O(5) [− <i>x</i> +2, − <i>y</i> +1, − <i>z</i> +1]
O(2)–H(3W)	0.83	1.98	164.4	2.785(4)	O(13) [− <i>x</i> +2, − <i>y</i> +1, − <i>z</i> +2]
O(2)–H(4W)	0.83	2.15	139.0	2.825(4)	O(11) [<i>x</i> +1, <i>y</i> , <i>z</i>]
O(2)–H(4W)	0.83	2.50	113.0	2.930(4)	O(3)
O(3)–H(5W)	0.83	1.91	162.8	2.714(4)	O(16) [<i>x</i> , <i>y</i> +1, <i>z</i>]
O(3)–H(6W)	0.83	1.97	171.5	2.790(4)	O(16) [− <i>x</i> +2, − <i>y</i> , − <i>z</i> +1]
O(4)–H(7W)	0.83	1.94	174.5	2.762(4)	O(6) [<i>x</i> −1, <i>y</i> −1, <i>z</i>]
O(4)–H(8W)	0.83	1.99	168.7	2.807(4)	O(10) [− <i>x</i> +1, − <i>y</i> +1, − <i>z</i> +1]
O(5)–H(9W)	0.83	2.11	161.6	2.904(4)	O(9) [<i>x</i> +1, <i>y</i> , <i>z</i>]
O(5)–H(10W)	0.83	1.96	158.8	2.748(4)	O(12) [<i>x</i> , <i>y</i> , <i>z</i> −1]
O(6)–H(12W)	0.83	2.10	126.3	2.678(5)	O(15) [<i>x</i> , <i>y</i> +1, <i>z</i>]
O(6)–H(12W)	0.83	2.15	156.6	2.933(5)	O(14) [<i>x</i> , <i>y</i> +1, <i>z</i>]
O(7)–H(13W)	0.83	1.96	164.9	2.765(4)	O(6)
O(7)–H(14W)	0.83	1.89	162.0	2.689(4)	O(11) [− <i>x</i> +1, − <i>y</i> +2, − <i>z</i> +1]
O(8)–H(15W)	0.83	1.99	161.5	2.788(4)	O(5)
O(8)–H(16W)	0.83	1.84	176.6	2.664(4)	O(13) [− <i>x</i> +1, − <i>y</i> +1, − <i>z</i> +1]
O(9)–H(17W)	0.83	1.91	164.2	2.718(4)	O(4) [<i>x</i> , <i>y</i> +1, <i>z</i>]
O(9)–H(18W)	0.83	1.97	169.2	2.794(4)	O(4) [− <i>x</i> , − <i>y</i> +1, <i>z</i>]

Acknowledgement

This work is supported by *National Natural Science Foundation of China* (20662007, 20961007).

References

- [1] X. J. Luan, Y. C. Chu, Y. Y. Wang, D. S. Li, P. Liu, Q. Z. Shi, *Cryst. Growth Des.* **2006**, *6*, 812–814.
- [2] X. Y. Cao, J. Zhang, Z. J. Li, J. K. Cheng, Y. G. Yao, *CrystEngComm* **2007**, *9*, 806–814.
- [3] H. L. Gao, L. Yi, B. Ding, H. S. Wang, P. Cheng, D. Z. Liao, S.-P. Yan, *Inorg. Chem.* **2006**, *45*, 481–483.
- [4] H. Ren, T. Y. Song, J. N. Xu, S. B. Jing, Y. Yu, P. Zhang, L. R. Zhang, *Cryst. Growth Des.* **2009**, *9*, 105–112.
- [5] F. Luo, Y. X. Che, J. M. Zheng, *J. Mol. Struct.* **2008**, *873*, 69–72.
- [6] X. Shi, G. S. Zhu, Q. R. Fang, G. Wu, G. Tian, R. W. Wang, D. L. Zhang, M. Xue, S. L. Qiu, *Eur. J. Inorg. Chem.* **2004**, 185–191.
- [7] S. Q. Ma, J. M. Simmons, D. F. Sun, D. Q. Yuan, H. C. Zhou, *Inorg. Chem.* **2009**, *48*, 5263–5268.
- [8] J. N. Moorthy, R. Natarajan, P. Venugopalan, *J. Org. Chem.* **2005**, *70*, 8568–8571.
- [9] Y. H. Zhao, H. B. Xu, K. Z. Shao, Y. Xing, Z. M. Su, J. F. Ma, *Cryst. Growth Des.* **2007**, *7*, 513–520.
- [10] R. H. Wang, F. L. Jiang, L. Han, Y. Q. Gong, Y. F. Zhou, M. C. Hong, *J. Mol. Struct.* **2004**, *699*, 79–84.
- [11] X. D. Guo, G. S. Zhu, F. X. Sun, Z. Y. Li, X. J. Zhao, X. T. Li, H. C. Wang, S. L. Qiu, *Inorg. Chem.* **2006**, *45*, 2581–2587.
- [12] L. J. Barbour, G. W. Orr, J. L. Atwood, *Nature* **1998**, *393*, 671–673.
- [13] X. Luan, Y. Chu, Y. Wang, D. Li, P. Liu, Q. Shi, *Cryst. Growth Des.* **2006**, *6*, 812–814.
- [14] R. Ludwig, *Angew. Chem. Int. Ed.* **2001**, *40*, 1809–1827.
- [15] T. Li, F. Li, Y. Wang, W. Bi, X. Li, R. Cao, *Inorg. Chim. Acta* **2007**, *360*, 3771–3776.
- [16] Y. C. Qiu, C. Daiguebonne, J. Q. Liu, R. H. Zeng, N. Kerbellec, H. Deng, O. Guillou, *Inorg. Chim. Acta* **2007**, *360*, 3265–3271.
- [17] S. Neogi, J. A. R. Navarro, P. K. Bharadwaj, *Cryst. Growth Des.* **2008**, *8*, 1554–1558.
- [18] X. L. Hong, Y. Z. Li, H. M. Hu, Y. Pan, J. F. Bai, X. Z. You, *Cryst. Growth Des.* **2006**, *6*, 1221–1226.
- [19] L. Tang, D. S. Li, F. Fu, Y. P. Wu, Y. Y. Wang, H. M. Hu, E. B. Wang, *J. Mol. Struct.* **2008**, *888*, 344–353.
- [20] S. N. Wang, J. F. Bai, H. Xing, Y. Z. Li, Y. Song, Y. Pan, M. Scheer, X. Z. You, *Cryst. Growth Des.* **2007**, *7*, 747–754.
- [21] H. T. Xu, R. J. Wang, Y. D. Li, *J. Mol. Struct.* **2004**, *688*, 1–3.
- [22] X. J. Zheng, L. P. Jin, S. Gao, *Inorg. Chem.* **2004**, *43*, 1600–1602.
- [23] F. Q. Wang, X. J. Zheng, Y. H. Wan, C. Y. Sun, Z. M. Wang, K. Z. Wang, L. P. Jin, *Inorg. Chem.* **2007**, *46*, 2956–2958.
- [24] C. Serre, F. Millange, C. Thouvenot, M. Noguès, G. Marsolier, D. Louër, G. Férey, *J. Am. Chem. Soc.* **2002**, *124*, 13519–13526.
- [25] Y. N. Gong, C. B. Liu, D. H. Huang, Z. Q. Xiong, *Z. Kristallogr., NCS* **2009**, *224*, 421–422.
- [26] C. Y. Ao, C. B. Liu, L. S. Yan, *Z. Kristallogr., NCS* **2009**, *224*, 179–180.
- [27] X. F. Wang, C. B. Liu, D. H. Huang, Z. Q. Xiong, *Acta Crystallogr., Sect. E* **2009**, *65*, m764–m765.
- [28] D. Eisenberg, W. Kauzmann, *The Structure and Properties of Water*, Oxford University Press, New York, **1969**.
- [29] S. S. Tan, H. L. Wen, C. B. Liu, X. P. Peng, *Z. Kristallogr., NCS* **2007**, *222*, 137–138.
- [30] G. M. Sheldrick, *SHELXS 97*, Program for Crystal Structure Solution, University of Göttingen, Göttingen, Germany, **1997**.
- [31] G. M. Sheldrick, *SHELXL 97*, Program for Crystal Structure Refinement, University of Göttingen, Göttingen, Germany, **1997**.

Received: June 2, 2010

Published Online: October 21, 2010